

Trigonometrically Extended Cornell Potential and Deconfinement

M. Kirchbach and C. Compean

Instituto de Física, Universidad Autónoma de San Luis Potosí, Av. Manuel Nava 6,
San Luis Potosí, S.L.P. 78290, México

Abstract. Non-perturbative methods of effective field theory such like Lattice QCD have allowed to establish connection between the QCD Lagrangian and quark potential models, a prominent outcome being the Cornell (linear plus Coulomb) potential. In being quite successful in explaining properties of heavy flavor hadrons, be them quarkonia or baryons, this potential has been found less spectacular in the description of the non-strange baryons, the nucleon and the Δ . This behavior indicates that the one-gluon exchange (giving rise to the inverse distance part) and the flux-tube interaction (responsible for the linear term) do not fully account for the complexity of the dynamics of three light quarks. Very recently the Cornell potential which is of infinite range has been upgraded by us toward an exactly solvable trigonometric potential of finite range that interpolates between the inverse-distance and the infinite wells while passing through a region of linear growth, a reason for which it contains the inverse distance and linear potentials as first terms in its Taylor series decomposition. We here first made the point that the upgraded Cornell potential can be viewed as the exact counterpart on a curved space to a flat space $1/r$ potential, a circumstance that equips it by two simultaneous symmetries, $SO(4)$, and $SO(2, 1)$. These allow to place the trigonometric confinement potential in the context of AdS_5/CFT correspondence and thus to establish the link of the algebraic aspects of the latter to QCD potentiology. Next we report that the above potential when employed in the quark-diquark system, provides a remarkably adequate description of both nucleon and Δ spectra and the proton mean square charge radius as well, and moreover implies an intriguing venue toward quark deconfinement as a shut-down of the curvature considered as temperature dependent.

1 Introduction

Significant progress in understanding hadron properties has been reached through the elaboration of the connection between the QCD Lagrangian and the potential models as deduced within the framework of effective field theories [1, 2] and especially through the non-perturbative methods such as lattice simulations, the most prominent outcome being the linear plus Coulomb confinement potential [3, 4]. The potentials derived from the QCD Lagrangian have been most successful in the description of heavy quarkonia and heavy baryon properties [5]. Although the Cornell potential has found applications also in nucleon and Δ quark models [6], the provided level of quality in the description of the non-strange sector stays below the one reached for the heavy flavor sector. This behavior indicates that the one gluon exchange (giving rise to the Coulomb-like term) and of the flux-tube interaction (associated with the linear part) do not fully account for the complexity of the dynamics

of three light quarks. Various improvements have been under consideration in the literature such as screening effects in combination with spin-spin forces (see [7] and reference's therein).

Very recently, the Cornell potential has been upgraded by us in [8] through its extension toward an exactly solvable (in the sense of the Schrödinger equation, or, the Klein-Gordon equation with equal scalar and vector potentials) trigonometric quark confinement potential. The latter has the property of interpolating between a Coulomb-like and an infinite well while passing through a region of linear growth, and was shown to provide a remarkably good description of the spectra of the non-strange baryons, the nucleon and the Δ , considered as quark-diquark systems, and of the proton charge radius as well [8].

The potential under discussion is of infinite depth and has only bound states which diagonalize the $SO(4)$ Casimir operator of the four-dimensional angular momentum. Alternatively, same states diagonalize also, under certain conditions to be discussed below, the three dimensional pseudo-angular momentum, the Casimir operator of $SO(2, 1)$. The first symmetry is embedded in the de Sitter group, $SO(1, 4)$, which by-itself is a subgroup of the conformal group $SO(2, 4)$ according to the reduction chain,

$$SO(2, 4) \supset SO(1, 4) \supset SO(4) \supset SO(3) \supset SO(2),$$

$$K \qquad l \qquad m. \qquad (1)$$

Here, K , l , and m are the respective four-, three- and two-dimensional angular momenta, $l = 0, 1, 2, \dots, K$, and $m = -l, \dots, 0, \dots, +l$. Alternatively, the $SO(2, 1)$ symmetry is part of the reduction chain of the anti-de Sitter group, $SO(2, 3)$,

$$SO(2, 3) \supset SO(2, 1) \supset SO(2),$$

$$j \qquad m'. \qquad (2)$$

Here, j is the so called Bargmann index that fixes the eigenvalues of the pseudo-angular momentum, $\mathcal{J}^2 = J_x^2 + J_y^2 - J_z^2$ as $\mathcal{J}^2|jm'\rangle = j(1-j)|jm'\rangle$, and m' is the J_z eigenvalue, $J_z|jm'\rangle = m'|jm'\rangle$, unlimited from above according to $m' = j, j+1, j+2, \dots$. The group symmetries under discussion appear within the context of a Schrödinger equation written in different variables [9, 10].

The first goal of the present contribution is to draw attention to the fact that the $SO(4)$ symmetry of the potential under discussion is well understood in terms of the solution to the Laplace-Beltrami equation on a three-dimensional sphere of constant radius, S_R^3 , embedded in a four-dimensional flat Euclidean space, E_4 , or, alternatively, in an Euclidean anti-de Sitter space.

The two symmetries are especially interesting in connection with a development initiated by [11] according to which a maximal supersymmetric Yang-Mills conformal field theory (CFT) in four dimensional Minkowski space is equivalent to a type IIB closed superstring theory in ten dimensions described by the product manifold

$AdS_5 \times S^5$. More recently, the correspondence between string theory in ten dimensional anti-de Sitter space and $SO(4, 2)$ invariant conformal Yang-Mills theories, so called AdS_5/CFT correspondence, has been adapted in [12] to the description of hadron properties.

We here emphasize that the $SO(4)$ and $SO(2, 1)$ symmetries of the “curved” potential are in line with the algebraic aspects of the AdS_5/CFT correspondence as visible from Eqs. (2) and (1) thus establishing a link of the latter to QCD potentiology.

However, it is important to be aware of the fact that the algebraic AdS_5/CFT criteria alone are not sufficient to fix uniquely the potential. One has to complement them by the requirement on compatibility with the QCD Lagrangian too, a condition which imposes severe restrictions on the allowed potential shapes.

Our next point is that it is precisely the trigonometrically extended Cornell potential, treated as quark-diquark potential, the one that meets best both the AdS_5/CFT and QCD criteria and provides the link between them. Predicted degeneracy patterns and level splitting are such that none of the observed N states drops out from the corresponding systematics which also applies equally well to the Δ spectra (except accommodation of the hybrid $\Delta(1600)$). The scenario provides a remarkable description of the proton charge electric form-factor too and moreover implies a deconfinement mechanism as a shut-down of the curvature considered as temperature dependent.

2 The “Curved” Cornell Potential

Around 1941 Schrödinger had the idea to solve the quantum mechanical Coulomb problem in the cosmological context of Einstein’s closed universe, i.e. on the three dimensional (3D) hypersphere, S_R^3 , of a constant radius R [13]. In order to construct the counterpart of the flat-space inverse distance potential on S_R^3 Schrödinger had to solve the corresponding four-dimensional Laplace-Beltrami equation. In result, after some straightforward algebra, he found the following potential

$$\mathcal{V}(\chi) = c \cot \chi + \kappa \frac{\hbar^2 l(l+1)}{2\mu \sin^2 \chi}, \quad \kappa = \frac{1}{R^2}. \quad (3)$$

Here χ stands for the second polar angle in E_4 , and the \csc^2 term describes the centrifugal barrier on S_R^3 . Schrödinger’s prime result, the presence of curvature provokes that the orbiting particle appears confined within a trigonometric potential of infinite depth and the hydrogen spectrum shows only bound states. This is a very interesting situation in so far as in E_4 the rôle of the radial coordinate of infinite range in ordinary flat space, $0 < r < \infty$, has been taken by the angular variable, χ , of finite range. In other words, while the harmonic potential in E_3 is a central one, in E_4 it is non-central. Moreover,

the inverse distance potential of finite depth in E_3 is converted to an infinite barrier and therefore to a confinement potential in the higher dimensional E_4 space, a property of fundamental importance throughout the paper. Stated differently, confinement phenomena can be associated with infinite barriers due to curvature.

An especially interesting observation was that the $O(4)$ degeneracy of the levels observed in the flat space H atom spectrum was preserved by the curved space spectrum too in the sense that also there the levels could be labeled by the standard atomic indices n , l , and m , and the energy depended on n alone.

The simplest barrier of such a nature is the manifestly $O(4)$ symmetric S_R^3 centrifugal barrier, $U_l(\chi, \kappa) = \kappa \frac{\hbar^2 l(l+1)}{2\mu \sin^2 \chi}$. Indeed, the angular part, \square_Ω , of the four-dimensional Laplacian, \square , relates to the operator of the four-dimensional angular momentum, here denoted by \mathcal{K}^2 ,¹ according to, $\square_\Omega = -\frac{1}{R^2}\mathcal{K}^2$, whose action on the states is given by [14]

$$\mathcal{K}^2|Klm\rangle = K(K+2)|Klm\rangle. \quad (4)$$

Therefore, the corresponding energy spectrum has to be, $E_K^{(c=0)}(\kappa) = \kappa \frac{\hbar^2}{2\mu} K(K+2)$. When cast in terms of $n = K+1$, the latter spectrum becomes $E_n^{(c=0)}(\kappa) = \kappa \frac{\hbar^2}{2\mu} (n^2 - 1)$, which coincides in form (though not in degeneracies) with the spectrum of a particle confined within an infinitely deep spherical quantum-box well. Then n acquires meaning of principal quantum number. The complete solutions of Eq. (4) especially on the unit hypersphere are text-book knowledge [14, 15] and are the well known hyper-spherical harmonics, $|Klm\rangle = Z_{Klm}(\chi, \theta, \varphi) = \mathcal{S}_{Kl}(\chi, \kappa = 1)Y_l^m(\theta, \varphi)$, where \mathcal{S}_{Kl} contain the Gegenbauer polynomials.

In general, various potentials in conventional flat E_3 space can be constructed as images to $\mathcal{V}(\chi)$ in Eq. (3). Their explicit forms are determined by the choice of coordinates on S_R^3 which shape the line element, ds . The general expression of the line element in the space under consideration and in hyper-spherical coordinates, $\Omega = \{\chi, \theta, \varphi\}$, reads

$$ds^2 = \frac{1}{\kappa} [d\chi^2 + \sin^2 \chi (d\theta^2 + \sin^2 \theta d\varphi^2)]. \quad (5)$$

Upon the variable substitution, $\chi = f(r)$, restricted to $0 \leq f(r) \leq \pi$, Eq. (5) takes the form

$$ds^2 = D^2(r, \kappa) \frac{dr^2}{r^2} + \mathcal{R}^2(r, \kappa) (d\theta^2 + \sin^2 \theta d\varphi^2), \quad (6)$$

¹ The analogue on the two-dimensional sphere of a constant radius $r = a$ is the well known relation $\vec{\nabla}^2 = -\frac{1}{a^2}L^2$.

where $D(r, \kappa) \equiv \frac{r}{\sqrt{\kappa}} f'(r)$, and $\mathcal{R}(r, \kappa) \equiv \frac{\sin f(r)}{\sqrt{\kappa}}$ are usually referred to as “gauge metric tensor” and “scale factor”, respectively [16]. Changing variable correspondingly in the associated Schrödinger equation is standard and various choices for $f(r)$ give rise to a variety of radial equations in ordinary flat space with effective potentials which are not even necessarily central. All these equations, no matter how different that may look, are of course equivalent, they have same spectra, and the transition probabilities between the levels are independent on the choice for $f(r)$. Nonetheless, some of the scenarios provided by the different choices for $f(r)$ can be more efficient in the description of particular phenomena than others.

Precisely here lies the power of the curvature concept as the common prototype of confinement phenomena of different disguises. In the following we shall present one typical example for $f(r)$.

2.1 The $D(r, \kappa) = \pi r$ Gauge and the Upgraded Cornell Potential

An especially simple and convenient parametrization of the χ variable in terms of r , also used by Schrödinger [13] and corresponding to the $D(r) = \pi r$ gauge is

$$\chi = \frac{r}{R}\pi \equiv \frac{r}{d}, \quad d = \frac{R}{\pi}, \quad \frac{r}{R} \in [0, 1], \quad \kappa \rightarrow \tilde{\kappa} = \frac{1}{d^2}. \quad (7)$$

Here, the length parameter d assumes the rôle of rescaled hyper-radius. Correspondingly, in this particular gauge, the place of the genuine curvature, $\kappa = 1/R^2$, is taken by the rescaled one, $\tilde{\kappa} = 1/d^2$. Setting now $c = -2G\sqrt{\tilde{\kappa}}$, amounts to the following radial Schrödinger equation,

$$\left[-\tilde{\kappa} \frac{\hbar^2}{2\mu} \frac{d^2}{d(r\sqrt{\tilde{\kappa}})^2} + \mathcal{V}(r\sqrt{\tilde{\kappa}}, \tilde{\kappa}) \right] X(r\sqrt{\tilde{\kappa}}, \tilde{\kappa}) = \left(E(\tilde{\kappa}) + \frac{\hbar^2}{2\mu} \tilde{\kappa} \right) X(r\sqrt{\tilde{\kappa}}, \tilde{\kappa}),$$

$$\mathcal{V}(r\sqrt{\tilde{\kappa}}, \tilde{\kappa}) = \tilde{\kappa} \frac{\hbar^2}{2\mu} \frac{l(l+1)}{\sin^2(r\sqrt{\tilde{\kappa}})} - 2G\sqrt{\tilde{\kappa}} \cot(r\sqrt{\tilde{\kappa}}). \quad (8)$$

A similarly shaped potential is managed by SUSYQM [17] under the name of Rosen-Morse I. The essential difference between Rosen-Morse I and $\mathcal{V}(r\sqrt{\tilde{\kappa}}, \tilde{\kappa})$ is the suppression of the curvature in the former and its treatment as a central potential in ordinary flat space. Instead, we here shall treat $\mathcal{V}(r\sqrt{\tilde{\kappa}}, \tilde{\kappa})$ consequently as a “curved” and maintain intact the S_R^3 volume in all integrals to appear.

It is now quite instructive to expand $\mathcal{V}(r\sqrt{\tilde{\kappa}}, \tilde{\kappa})$ in a Taylor series. In so doing, one finds the following approximation,

$$-2G\sqrt{\tilde{\kappa}} \cot r\sqrt{\tilde{\kappa}} + \tilde{\kappa} \frac{\hbar^2}{2\mu} \frac{l(l+1)}{\sin^2(r\sqrt{\tilde{\kappa}})} \approx -\frac{2G}{r} + \frac{2G\tilde{\kappa}}{3} r + \frac{\hbar^2}{2\mu} \frac{l(l+1)}{r^2}, \quad (9)$$

$$\text{with } \tilde{\kappa} = \frac{1}{d^2} = \frac{\pi^2}{R^2}.$$

Therefore, the finite range potential, $\mathcal{V}(r\sqrt{\tilde{\kappa}}, \tilde{\kappa})$, is the exactly solvable *trigonometric extension to the infinite range Cornell* potential, to be referred to as TEC potential.

Besides Schrödinger, Eq. (8) has been solved by various authors using different schemes. The solutions obtained in [18] are built on top of Jacobi polynomials of imaginary arguments and parameters that are complex conjugate to each other, while Ref. [19] expands the wave functions of the interacting case in the free particle basis. The most recent construction in our previous work [20] instead relies upon real Romanovski polynomials. In the χ variable in Eq. (7) our solutions to Eq. (8) take the form,

$$X_{(Kl)}(\chi, \tilde{\kappa}) = N_{(Kl)} \sin^{K+1} \chi e^{-\frac{b\chi}{\tilde{\kappa}+1}} R_{K-l}^{(\frac{2b}{\tilde{\kappa}+1}, -(K+1))}(\cot \chi), \quad b = \frac{2\mu G}{\sqrt{\tilde{\kappa}}\hbar^2},$$

$$K = 0, 1, 2, \dots, \quad l = 0, 1, \dots, K, \quad (10)$$

where $N_{(Kl)}$ is a normalization constant. The $R_n^{(\alpha, \beta)}(\cot \chi)$ functions are the non-classical Romanovski polynomials [21, 22] which are defined by the following Rodrigues formula,

$$R_n^{(\alpha, \beta)}(x) = e^{\alpha \cot^{-1} x} (1+x^2)^{-\beta+1} \frac{d^n}{dx^n} e^{-\alpha \cot^{-1} x} (1+x^2)^{\beta-1+n}, \quad (11)$$

where $x = \cot r\sqrt{\tilde{\kappa}}$ (see Ref. [23] for a recent review).

The energy spectrum of $\mathcal{V}(r\sqrt{\tilde{\kappa}}, \tilde{\kappa})$ is calculated as

$$E_K(\tilde{\kappa}) = -\frac{G^2}{\hbar^2} \frac{1}{(K+1)^2} + \tilde{\kappa} \frac{\hbar^2}{2\mu} ((K+1)^2 - 1), \quad l = 0, 1, 2, \dots, K. \quad (12)$$

Giving $(K+1)$ the interpretation of a principal quantum number $n = 0, 1, 2, \dots$ (as in the H atom), one easily recognizes that the energy in Eq. (12) is defined by the Balmer term and its inverse of opposite sign, thus revealing $O(4)$ as dynamical symmetry of the problem. Stated differently, particular levels bound within different potentials (distinct by the values of l) carry same energies and align to levels (multiplets) characterized, similarly to the free case in Eq. (4), by the four dimensional angular momentum, K . The K -levels belong to the irreducible $O(4)$ representations of the type $(\frac{K}{2}, \frac{K}{2})$. When the confined particle carries spin-1/2, as is the case of electrons in quantum dots, or quarks in baryons, one has to couple the spin, i.e. the $(\frac{1}{2}, 0) \oplus (0, \frac{1}{2})$ representation, to the previous multiplet, ending up with the (reducible) $O(4)$ representation

$$|Klm, s = \frac{1}{2}\rangle = \left(\frac{K}{2}, \frac{K}{2}\right) \otimes \left[\left(\frac{1}{2}, 0\right) \oplus \left(0, \frac{1}{2}\right)\right]. \quad (13)$$

This representation contains K parity dyads and a state of maximal spin, $J_{\max} = K + \frac{1}{2}$, without parity companion and of either positive ($\pi = +$) or, negative ($\pi = -$) parity,

$$\frac{1^\pm}{2}, \dots, \left(K - \frac{1}{2}\right)^\pm, \left(K + \frac{1}{2}\right)^\pi \in |Klm, s = \frac{1}{2}\rangle. \quad (14)$$

As we shall see below this scenario turns to be remarkably adequate for the description of non-strange baryon structure.

3 S_R^3 Potentiology: The Baryons

3.1 The Nucleon Spectrum in the $SO(4)$ Symmetry Scheme

The spectrum of the nucleon continues being enigmatic despite the long history of the respective studies (see Refs. [24, 25] for recent reviews). Unprejudiced inspection of the data reported by the Particle Data Group [26] reveals a systematic degeneracy of the excited states of the baryons of the best coverage, the nucleon (N) and the $\Delta(1232)$. Our case is that

– levels and level splittings of the nucleon and Δ spectra match remarkably well the spectrum in Eq. (12).

1. The N and Δ spectra: The measured nucleon resonances with masses below 2.5 GeV fall into the three $K = 1, 3, 5$ levels in Eq. (14) with only the two F_{17} and $H_{1,11}$ states still “missing”, a systematics anticipated earlier by one of us (M.K.) in Refs. [27] on the basis of pure algebraic considerations. Moreover, the level splittings follow with an amazing accuracy Eq. (12). The nucleon spectrum in the quark-diquark picture of internal structure, shown in Figure 1, is fitted by the following parameters of the “curved” potential in Eq. (8),

$$\mu = 1.06 \text{ fm}^{-1}, \quad G = 237.55 \text{ MeV} \cdot \text{fm}, \quad d = 2.31 \text{ fm}. \quad (15)$$

Almost same set of parameters, up to a modification of d to $d = 3 \text{ fm}$, fits the $\Delta(1232)$ spectrum, which exhibits exactly same degeneracy patterns, and from which only the three P_{31}, P_{33} , and D_{33} states from the $K = 5$ level are “missing”. Remarkably, none of the reported states, with exception of the $\Delta(1600)$ resonance, presumably a hybrid, drops from the systematics. The unnatural parity of the $K = 3, 5$ levels requires a pseudoscalar diquark. For that one has to account for an 1^- internal excitation of the diquark which, when coupled to its maximal spin 1^+ , can produce a pseudoscalar in one of the possibilities. The change of parity from natural to unnatural can be given the interpretation of a chiral phase transition in baryon spectra. Levels with $K = 2, 4$ have been attributed to entirely “missing” resonances in both the N and Δ spectra. To them, natural parities have been assigned on the basis of a detailed analysis of the $(1p-1h)$ Hilbert space of three quarks and its decomposition in the $|Klm, s = \frac{1}{2}\rangle$ basis [27]. We predict a total of 33 unobserved resonances of a dominant quark-diquark configurations in the N and $\Delta(1232)$ spectra with masses below $\sim 2500 \text{ MeV}$, much less but any other of the traditional models.

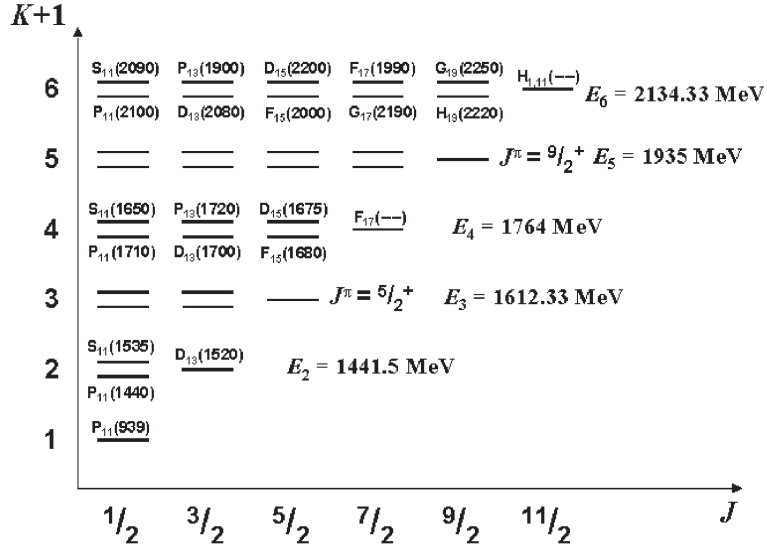


Figure 1. Assignments of the reported N excitations to the K levels of the S_R^3 potential, $\mathcal{V}(r\sqrt{\tilde{\kappa}}, \tilde{\kappa})$, in Eq. (8), taken as the quark-diquark confinement potential. The potential parameters are those from Eq. (15). Double bars represent parity dyads, single bars the unpaired states of maximum spin. The notion $L_{2I,2J}(-)$ has been used for resonances “missing” from a level. The model predicts two more levels of maximal spins $J^\pi = 5/2^+$, and $J^\pi = 9/2^+$, respectively, which are completely “missing”. In order not to overload the figure with notations, the names of the resonances belonging to them have been suppressed. The predicted energy at rest (equal to the mass) of each level is given to its most right.

In our previous work [8], the potential in Eq. (8) has been considered in the spirit of SUSYQM as a *central two-parameter* potential in E_3 and without reference to S_R^3 , a reason for which the values of the parameter accompanying the csc^2 term had to be taken as integer *ad hoc* and for the only sake of a better fit to the spectra, i.e., without any deeper justification. Instead, in the present work,

we fully recognize that the higher dimensional potential $\mathcal{V}(\chi, \kappa)$ in Eq. (3), which acts as the prototype of Rosen-Morse I, is a *non-central one-parameter* potential in which the strength of the csc^2 term, the centrifugal barrier on S_R^3 , is uniquely fixed by the eigenvalues of underlying three-dimensional angular momentum.

3.2 The Nucleon Spectrum in the $SO(2, 1)$ Symmetry Scheme

As already announced in the introduction, the energy spectrum in Eq. (12) can equivalently be cast in terms of the eigenvalues of the $SO(2, 1)$ Casimir, the pseudo-angular momentum operator, \mathcal{J}^2 [9, 10]. At first glance, it is not obvious how to re-express in terms of $SO(2, 1)$ quantum numbers the general two-term energy formula

in Eq. (12) that contains both the quadratic and inverse quadratic eigenvalues of the $SO(4)$ Casimir. An immediate option would be to nullify the potential strength, i.e. setting $G = 0$, which turns one back to the free particle on the hypersphere. In this case only the quadratic terms survives which is easily equivalently rewritten to

$$E_{m'}(\tilde{\kappa}) = \tilde{\kappa} \frac{\hbar^2}{2\mu} \left((m')^2 - 1 \right), \quad j = l + 1, \quad m' = j + n, \quad (16)$$

where l is the ordinary angular momentum label, while n is the radial quantum number (it equals the order of the polynomial shaping the wave function labeled by K in Eq. (10)). It is obvious that the degeneracy patterns in the $SO(2, 1)$ spectrum designed in this manner are same as the $SO(4)$ ones.

Perhaps nothing expresses the $SO(2, 1)/SO(4)$ symmetry correspondence better but this extreme case in which the manifestly $SO(4)$ symmetric centrifugal energy on the $3D$ hypersphere is cast in terms of $SO(2, 1)$ quantum numbers of pseudo-angular momentum.

Although the bare $l(l + 1) \csc^2 \chi$ potential is algebraically in line with AdS_5/CFT correspondence, it completely misses the perturbative aspect of QCD dynamics. The better option for getting rid of the inverse-quadratic term in Eq. (12) is to permit K dependence of the potential strength and choose $G = g(K + 1)$ with g being a new free parameter. Such a choice (up to notational differences) has been suggested in [28] in the context of SUSYQM. If so, then the energy takes the form

$$E_{m'}(\tilde{\kappa}) = -g^2 \frac{\hbar^2}{2\mu} + \tilde{\kappa} \frac{\hbar^2}{2\mu} \left((m')^2 - 1 \right), \quad m' = 1, 2, 3, \dots \quad (17)$$

The above manipulation does not affect the degeneracy patterns as it only provokes a shift in the spectrum by a constant. Compared to Eq. (16) the new choice allows the former inverse quadratic term to still keep presence as a contribution to the energy depending on a free constant parameter, g . In this manner, the $SO(2, 1)$ energy spectrum continues being described by a two-term formula, a circumstance that allows for a best fit to the $SO(4)$ description.

Once having ensured that the $SO(2, 1)$ and $SO(4)$ spectra share same degeneracy patterns, one is only left with the task to check consistency of the level splittings predicted by the two schemes. Comparison of Eqs. (12) and (17) shows that for the high-lying levels where the inverse quadratic term becomes negligible, both formulas can be made to coincide to high accuracy by a proper choice for g . That very g parameter can be used once again to fit the low lying levels to the $SO(4)$ description, now by a value possibly different from the previous one.

This strategy allows to make the $SO(2, 1)$ and $SO(4)$ descriptions of non-strange baryon spectra sufficiently close and establish the symmetry correspondence. In that manner we confirm our statement quoted in the introduction that the TEC potential is in line with both the algebraic aspects of AdS_5/CFT and QCD dynamics and provides a bridge between them.

3.3 The Proton Mean Square Charge Radius

In this section we shall test the potential parameters in Eq. (15) and the wave function in Eqs. (8), (10) in the calculation of the proton electric form-factor, the touchstone of any spectroscopic model. As everywhere through the paper, the internal nucleon structure is approximated by a quark-diquark configuration. In conventional three-dimensional flat space the electric form factor is defined in the standard way as the matrix element of the charge component, $J_0(\mathbf{r})$, of the proton electric current between the states of the incoming, \mathbf{p}_i , and outgoing, \mathbf{p}_f , electrons in the dispersion process,

$$G_E^p(|\mathbf{q}|) = \langle \mathbf{p}_f | J_0(\mathbf{r}) | \mathbf{p}_i \rangle, \quad \mathbf{q} = \mathbf{p}_i - \mathbf{p}_f. \quad (18)$$

The mean square charge radius is then defined in terms of the slope of the electric charge form factor at origin and reads,

$$\langle r^2 \rangle = -6 \frac{\partial G_E^p(|\mathbf{q}|)}{\partial |\mathbf{q}|^2} \Big|_{|\mathbf{q}|^2=0}. \quad (19)$$

On S_R^3 , the three-dimensional radius vector, \mathbf{r} , has to be replaced by, $\bar{\mathbf{r}}$ with $|\bar{\mathbf{r}}| = R \sin \chi = \sin \chi / \sqrt{\kappa}$. The evaluation of Eq. (18) as four-dimensional Fourier transform requires the four-dimensional plane wave,

$$e^{iq \cdot \bar{x}} = e^{i|\mathbf{q}||\bar{\mathbf{r}}| \cos \theta} = e^{i|\mathbf{q}| \frac{\sin \chi}{\sqrt{\kappa}} \cos \theta}, \quad |\bar{\mathbf{r}}| = R \sin \chi = \frac{\sin \chi}{\sqrt{\kappa}}. \quad (20)$$

The latter refers to a z axis chosen along the momentum vector (a choice justified in elastic scattering²), and a position vector of the confined quark having in general a non-zero projection on the extra dimension axis in E_4 .

The integration volume on S_R^3 is given by $\sin^2 \chi \sin \theta d\chi d\theta d\varphi$. The explicit form of the nucleon ground state wave function obtained from Eq. (10) in the χ variable reads

$$X_{(00)}(\chi, \tilde{\kappa}) = N_{(00)} e^{-b\chi} \sin \chi, \quad (21)$$

$$N_{(00)} = \frac{4b(b^2 + 1)}{1 - e^{-2\pi b}}, \quad b = \frac{2\mu G}{\sqrt{\tilde{\kappa}} \hbar^2}.$$

With that, the charge-density takes the form, $J_0(\chi, \tilde{\kappa}) = e_p |\psi_{\text{gst}}(\chi, \tilde{\kappa})|^2$, $e_p = 1$. In effect, Eq. (18) amounts to the calculation of the following integral,

$$G_E^p(|\mathbf{q}|, \tilde{\kappa}) = \sqrt{\tilde{\kappa}} \int_0^\pi d\chi \frac{(X_{(00)}(\chi, \tilde{\kappa}))^2 \sin(|\mathbf{q}| \frac{\sin \chi}{\sqrt{\tilde{\kappa}}})}{|\mathbf{q}| \sin \chi}, \quad (22)$$

where the dependence of the form factor on the curvature has been indicated explicitly. The integral is taken numerically and the resulting charge form factor of the proton is displayed in Figure 2 together with data.

² A consistent definition of the four-dimensional plane wave in E_4 would require an Euclidean q vector. However, for elastic scattering processes, of zero energy transfer, where $q_0 = 0$, the q vector can be chosen to lie entirely in E_3 , and be identified with the physical space-like momentum transfer.

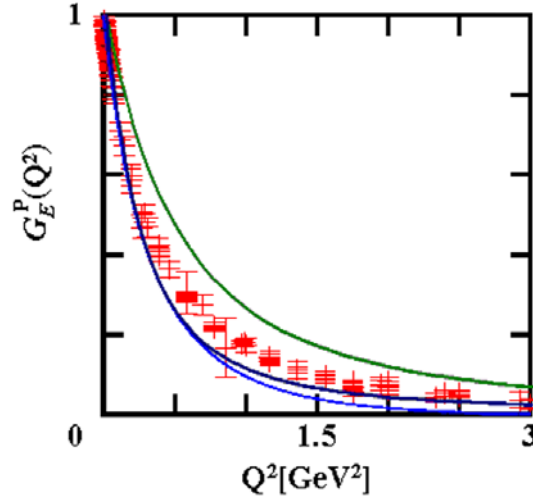


Figure 2. The electric charge form factor of the proton calculated for various curvature parameters. The upper line corresponds to the curvature as fitted to the nucleon spectrum, the curvature leading to the middle line has been fitted to the experimental value of the mean square of the charge radius, $\sqrt{\langle r^2 \rangle} = 0.87$ fm. The lowest line follows from a Bethe-Salpeter calculation based upon an instanton induced two-body potential and has been presented in Ref. [29]. Data compilation taken from [29].

4 Curvature Shut-Down: The Deconfinement

The presence of the curvature parameter in the trigonometrically extended Cornell confinement potential opens an intriguing venue toward deconfinement as a S_R^3 curvature shut-down. It can be shown that

high-lying bound states from the trigonometrically extended Cornell confinement potential approach scattering states of the Coulomb-like potential in ordinary flat space. Stated differently, the TEC confinement gradually fades away with vanishing curvature and allows for deconfinement.

In the direct $\kappa \rightarrow 0$ limit, the second term of the r.h.s. in Eq. (12) vanishes and the spectrum becomes the one of H atom-like bound states. In the softer $\sqrt{\kappa}K \rightarrow k$ (small κ , big K) limit, where “ k ” is a constant, the term in question approaches the scattering continuum. In effect, the $\mathcal{V}(\chi, \kappa)$ spectrum collapses down to the regular Coulomb-like potential,

$$E_K(\kappa) \xrightarrow{\kappa \rightarrow 0} -\frac{G^2}{\frac{\hbar^2}{2\mu}} \frac{1}{n^2} + \frac{\hbar^2}{2\mu} k^2, \quad l = 0, 1, 2, \dots, n-1. \quad (23)$$

The rigorous proof that also the wave functions of the complete TEC potential collapse to those of the corresponding Coulomb-like problem for vanishing curvature is a bit more involved and can be found in [19]. In other words,

as curvature goes down as it can happen because of its thermal dependence, confinement fades away, an observation that is suggestive of a deconfinement scenario controlled by the curvature parameter of the TEC potential.

Deconfinement as gradual flattening of space has earlier been considered by Takagi [30]. Compared to [30], our scheme brings the advantage that the flattening of space is paralleled by a temperature driven regression of the TEC potential in Eq. (8) to the flat Coulomb-like potential, and correspondingly, by the temperature driven regression of the TEC wave functions from the confined to the Coloumb-like wave-functions from the deconfined phases.

5 Summary

We emphasized importance of designing confinement phenomena in terms of infinite potential barriers emerging on curved spaces. Especially, quark confinement and QCD dynamics have been modeled in terms of a trigonometric potential of finite range that emerges as harmonic potential on the three-dimensional hypersphere of constant curvature, i.e., a potential that satisfies the Laplace-Beltrami equation there. The potential under consideration interpolates between the $1/r$ - and infinite wells while passing through a region of linear growth. This trigonometric confinement potential is exactly solvable at the level of the Schrödinger equation and moreover, contains the infinite range Cornell potential following from Lattice QCD and topological field theory as leading terms of its Taylor decomposition. When employed as a quark-diquark potential, it led to a remarkably adequate description of the N and Δ spectra in explaining their $O(4)/SO(2, 1)$ degeneracy patterns, level splittings, number of states, and proton electric charge-form factor. Moreover, the trigonometrically extended Cornell (TEC) potential, in carrying simultaneously the $SO(4)$ and $SO(2, 1)$ symmetries (as the H atom!), matches the algebraic aspects of AdS_5/CFT correspondence and establishes its link to QCD potentiology. A further advantage of the TEC potential is the possibility to employ its curvature parameter, considered as temperature dependent, as a driver of the confinement-deconfinement transition in which case the wave functions of the confined phase approach bound and scattering states of ordinary flat space $1/r$ potential.

All in all, we view the concept of curved spaces as a promising one especially within the context of quark-gluon dynamics.

Acknowledgments

One of us (M.K) acknowledges the organizers of the XXVII International Workshop on Nuclear Theory in the Rila Mountains, Bulgaria, for warm hospitality and excellent working conditions during the event.

Work supported by CONACyT-México under grant number CB-2006-01/61286.

References

1. G. S. Bali, *Wien 2000, Quark confinement and the hadron spectrum*, 209–220 (2000); e-Print: hep-ph/0010032.
2. N. Brambilla, A. Vairo, Th. Rosch, *Phys.Rev.D* **72**, 034021 (2005);
N. Brambilla, *AIP Conf.Proc.* **756**, 366–368 (2005).
3. T. T. Takahashi, H. Suganuma, Y. Nemoto, H. Matsufuru, *Phys. Rev. D* **65**, 114509-1–19 (2002).
4. E. Eichten, H. Gottfried, T. Kinoshita, K. D. Lane, T.M. Yan, *Phys. Rev. D* **17**, 3090–3117 (1978);
E. Eichten, H. Gottfried, T. Kinoshita, K. D. Lane, T.M. Yan, *Phys. Rev. D* **21**, 203–233 (1980).
5. Quarkonium Working Group (N. Brambilla *et al.*), *Heavy quarkonium physics*, CERN Yellow Report, CERN-2005-005, Geneva: CERN, (2005); e-Print: hep-ph/0412158.
6. P. Gonzalez, J. Vijande, A. Valcarce, H. Garcilazo, *Eur. Phys. J. A* **29**, 235–244 (2006).
7. H. Garcilazo, *Phys. Rev. C* **67**, 055203-1–9 (2003).
8. C. B. Compean, M. Kirchbach, *Eur. Phys. J. A* **33**, 1–4 (2007).
9. Brian G. Wybourne, *Classical groups for physicists* (Wiley-Inter-science, N.Y., 1974).
10. M. Novaes, *Revista Brasileira de Ensino de Fisica* **26**, 351–357 (2004).
11. J. Maldacena, *Adv. Theor. Math. Phys.* **2**, 231–252 (1998); *Int. J. Theor. Phys.* **38**, 1113–1133 (1999).
12. Guy F. de Téramond, S. J. Brodsky, *Phys. Rev. Lett.* **94**, 201601-1–4 (2005).
13. E. Schrödinger, *Proc. Roy. Irish Acad. A* **46**, 9–16 (1940).
14. Y. S. Kim, M. E. Noz, *Theory and application of the Poincaré group* (D. Reidel, Dordrecht, 1986).
15. Taco Nieuwenhuis, J. A. Tjon, *Few Body Syst.* **21**, 167–185 (1996).
16. A. A. Ismest’ev, *Sov. J. Nucl. Phys.* **52**, 1066–1076 (1990).
17. R. De, R. Dutt, U. Sukhatme, *J. Phys. A: Math. Gen.* **25**, L843–L850 (1992).
18. A. F. Stevenson, *Phys. Rev.* **59**, 842–843 (1941).
19. S. I. Vinitzky, L. G. Mardoian, G. S. Pogosyan, A. N. Sissakian, T. A. Strizh, *Phys. Atom. Nucl.* **56**, 321–327 (1993);
V. N. Pervushin, G. S. Pogosyan, A. N. Sissakian, S. I. Vinitzky, *Phys. Atom. Nucl.* **56**, 1027–1043 (1993).
20. C. B. Compean, M. Kirchbach, *J. Phys. A:Math.Gen.* **39**, 547–557 (2006).
21. E. J. Routh, *Proc. London Math. Soc.* **16**, 245 (1884).
22. V. Romanovski, *C. R. Acad. Sci. Paris*, **188**, 1023–1025 (1929).
23. A. Raposo, H. J. Weber, D. E. Alvarez-Castillo, M. Kirchbach, *C. Eur. J. Phys.* **5**, 253–284 (2007).
24. V. D. Burkert, T. S. H. Lee, *Int. J. Mod. Phys. E* **13**, 1035–1112 (2004).
25. S. S. Afonin, *Int. J. Mod. Phys. A* **22**, 4537–4586 (2007).
26. S. Eidelman *et al.*, *Phys. Lett. B* **592**, 1–1109 (2004).
27. M. Kirchbach, *Mod. Phys. Lett. A* **12**, 2373–2386 (1997);
M. Kirchbach, *Int. J. Mod. Phys. A* **15**, 1435–1451 (2000);
M. Kirchbach, M. Moshinsky, Yu. F. Smirnov, *Phys. Rev. D* **64**, 114005-1–11 (2001).
28. R. Koc, M. Koca, *J. Phys. A:Math.Gen.* **36**, 8105–8112 (2003).
29. B. Metsch, <http://www.itkp.uni-bonn.de/~metsch/jlab2004.pdf>.
30. F. Takagi, *Phys. Rev. D* **35**, 2226–2229 (1987).